BIOCHEMISTRY
including biophysical chemistry & molecular biology

ARTICLE

pubs.acs.org/biochemistry

Crystal Structures of Antibiotic-Bound Complexes of Aminoglycoside 2″-Phosphotransferase IVa Highlight the Diversity in Substrate Binding Modes among Aminoglycoside Kinases

Kun Shi,[†] Douglas R. Houston,[†,§] and Albert M. Berghuis*[,†,‡]

[†]Department of Biochemistry and [‡]Department of Microbiology and Immunology, Groupe de Recherche Axé sur la Structure des Protéines, McGill University, 3649 Promenade Sir William Osler, Montreal, Quebec H3G 0B1, Canada

ABSTRACT: Aminoglycoside 2″-phosphotransferase IVa [APH(2″)-IVa] is a member of a family of bacterial enzymes responsible for medically relevant resistance to antibiotics. APH(2″)-IVa confers high-level resistance against several clinically used aminoglycoside antibiotics in various pathogenic *Enterococcus* species by phosphorylating the drug, thereby preventing it from binding to its ribosomal target and producing a bactericidal effect. We describe here three crystal structures of APH(2″)-IVa, one in its apo form and two in complex with a bound antibiotic, tobramycin and kanamycin A. The apo structure was refined to a resolution of 2.05 Å, and the APH(2″)-IVa structures with tobramycin and kanamycin A bound were refined to resolutions of 1.80 and 2.15 Å, respectively. Comparison among the structures provides insight concerning the substrate selectivity of this enzyme. In particular, conformational changes upon substrate binding, involving rotational shifts of two distinct segments of the enzyme, are observed. These substrate-induced shifts may also rationalize the altered substrate preference of APH(2″)-IVa in comparison to those of other members of the APH(2″) subfamily, which are structurally closely related. Finally, analysis of the interactions between the enzyme and aminoglycoside reveals a distinct binding mode as compared to the intended ribosomal target. The differences in the pattern of interactions can be utilized as a structural basis for the development of improved aminoglycosides that are not susceptible to these resistance factors.

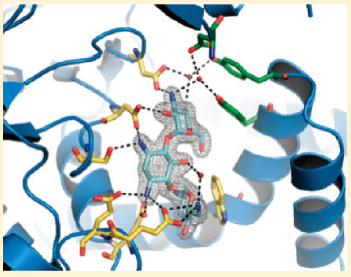

Bacterial resistance to antibiotics persists as a global threat to public health. Since the introduction of streptomycin against pulmonary tuberculosis some 65 years ago, aminoglycosides have remained an important class of bactericidal antibiotics.[1−3] Often used in combination with a β-lactam, aminoglycosides exert their effect by interacting with the A-site of bacterial 16S rRNA, thereby impairing the fidelity of protein translation and leading to the production of aberrant proteins.[4,5] Because of their extensive use both in clinical settings and on food-producing farm animals, resistant isolates are continually being discovered, including those of life-threatening species such as *Pseudomonas aeruginosa* and various pathogenic enterococci strains.[6,7]

Unlike streptomycin, the majority of aminoglycosides currently in clinical use are based on a 4,5- or 4,6-disubstituted 2-deoxystreptamine scaffold. By convention, the central 2-deoxystreptamine ring is termed ring B, with the 4-substituted aminocyclitol ring called ring A and any substituent on the 5 or 6 position called ring C. Variation among the numerous functional groups on rings A and C gives rise to the large repertoire of natural and semisynthetic aminoglycosides. Because the substituents on ring B are in equatorial positions, the resulting molecule adopts a roughly crescent-shaped conformation, where a convex and a concave side can be differentiated.

The major resistance mechanism for aminoglycoside antibiotics is the enzymatic modification of the drug, which leads to poor ribosome binding and decreased efficacy, by a series of proteins collectively termed the aminoglycoside-modifying enzymes. Among this large and growing group of enzymes, aminoglycoside *O*-phosphotransferases (APHs) catalyze the transfer of a phosphate group to specific hydroxyl groups on a wide variety of aminoglycosides, resulting in high-level resistance.[8] Within the APH family, those members that detoxify atypical aminoglycosides, including APH(4), APH(6), APH(9), APH(3″), and APH(7″), generally have a substrate spectrum limited to one drug, whereas those members that detoxify 4,5- or 4,6-disubstituted aminoglycosides, including APH(3′) and APH(2″), generally have a much broader substrate spectrum.[9] The structural basis underlying this difference in substrate specificity is presumably that the active site architectures of the first group have evolved to specifically accommodate the unique features of the respective atypical aminoglycoside. The second group, on the other hand, has exploited structural properties common to many 4,5- or 4,6-disubstituted aminoglycosides and thus evolved more promiscuous substrate-binding sites that enhance the versatility of the enzyme.

The APH(2″) subfamily currently consists of five structurally related phosphotransferases, which share limited sequence homology (~30%) and possess differences in substrate preferences.[10−13] Among them, APH(2″)-IVa has been found in approximately 16% of gentamicin-resistant enterococci isolates around the world.[12,14,15] Kinetic studies have shown that APH(2″)-IVa is

Received: May 13, 2011
Revised: June 16, 2011
Published: June 16, 2011

ACS Publications © 2011 American Chemical Society

also efficient at deactivating a number of other 4,6-disubstituted aminoglycosides, including tobramycin and kanamycin A, but is unable to modify any 4,5-disubstituted aminoglycosides.[16] The structure of the apo state has recently been reported, but data for substrate-bound states are lacking.[16] However, structural details have been reported for APH(2″)-IIa in its binary and ternary complexes.[17] In addition, various structures of four other members of the APH family, APH(4)-Ia, APH(9)-Ia, APH(3′)-IIa, and APH(3′)-IIIa, have been determined.[18−22] Combined, structural studies of APH enzymes reveal that despite a very low level of sequence identity [e.g., APH(2″)-IVa is 30 and 9% identical in sequence to APH(2″)-IIa and APH(3′)-IIIa, respectively] and diverse resistance profiles, they nevertheless display a remarkably similar three-dimensional fold. However, the similarity in structure and partially overlapping resistance profiles does not imply that these enzymes bind their antibiotic substrates similarly. For example, APH(2″)-IIa has been shown to bind aminoglycosides in a completely different orientation compared to APH(3′) enzymes.[17] Even within the APH(2″) enzymes, disparate substrate profiles and preferences suggest unique structural properties for each member of the family. For instance, APH(2″)-Ia is unique in that it can detoxify both 4,5- and 4,6-disubstituted aminoglycosides; APH(2″)-IIIa prefers tobramycin as a substrate, while APH(2″)-IVa is best able to phosphorylate gentamicin. Additionally, APH(2″)-IVa is the only member within its family that can utilize both ATP and GTP as a phosphate donor at comparable efficiencies.[23] Such differences impact the development of novel aminoglycosides and underline the necessity of understanding the structure of individual enzymes on an atomic level.

Here we report three crystal structures of APH(2″)-IVa, one substrate-free structure that is distinct from that previously reported and two in complex with either tobramycin or kanamycin A. These structures shed light on the substrate specificity of APH(2″)-IVa and reveal a degree of protein flexibility not commonly seen in APH enzymes. These results inform potential strategies for the design of next-generation aminoglycoside antibiotics that are less susceptible to drug resistance.

EXPERIMENTAL PROCEDURES

Cloning, Protein Expression, and Purification. The gene of native *aph(2″)-IVa*, kindly provided by J. Chow,[12] was cloned into expression vector pET22b(+) between the NdeI and HindIII restriction sites and transformed into competent *Escherichia coli* BL21(DE3) cells. A 20 mL starter culture was used to inoculate 1 L of LB medium supplemented with 100 μg/mL ampicillin. The culture was incubated at 37 °C with vigorous agitation until the optical density measured at 600 nm reached ∼0.6, at which time expression of APH(2″)-IVa was induced by the addition of 0.1 mM isopropyl β-D-thiogalactopyranoside and allowed to proceed at 15 °C overnight. Cells were harvested by centrifugation (6000*g* for 20 min at 4 °C), resuspended in 40 mL of a buffer consisting of 50 mM Tris-HCl (pH 8.5), 300 mM NaCl, and one EDTA-free protease inhibitor tablet, and lysed by sonication. The lysate was centrifuged (50000*g* for 30 min at 4 °C) and purified by Ni-NTA affinity chromatography in 50 mM Tris-HCl (pH 8.5) and 300 mM NaCl. After elution with a continuous imidazole gradient (0 to 500 mM), fractions were analyzed by sodium dodecyl sulfate−polyacrylamide gel electrophoresis (SDS−PAGE), and those containing the target protein were further purified by size-exclusion chromatography using a Superdex S-75 column equilibrated with 50 mM Tris-HCl (pH 8.5) and 300 mM NaCl. The purity and activity of the product were verified by SDS−PAGE and a previously established enzyme activity assay.[24]

Crystallization and Data Collection. Crystals of apo APH(2″)-IVa were grown at 4 °C using the hanging drop vapor diffusion method by equilibrating a 4 μL solution consisting of a 2 μL protein solution at 8 mg/mL and a 2 μL buffer solution of 200 mM NaCl and 15% (w/v) polyethylene glycol 2000 in 50 mM Tris-HCl (pH 8.5) against a reservoir containing 700 μL of the buffer solution. Crystals reach a maximal size of 0.5 mm × 0.1 mm × 0.1 mm within 2 weeks. Crystals were soaked in a buffer solution supplemented with 10% glycerol before data were collected under cryogenic conditions (−180 °C) on a Rigaku rotating copper anode X-ray generator. A total of 360 images with an oscillation angle of 1° were measured.

Crystals of binary complexes were grown at 4 °C using the sitting drop vapor diffusion method by combining 1.5 μL of a solution comprised of 6 mg/mL protein and 1.6 mM aminoglycoside antibiotic with 1.5 μL of 17% (w/v) polyethylene glycol 4000, 10% glycerol, and 5% 2-propanol in 50 mM HEPES (pH 7.5) and equilibrated against 40 μL of the latter in an MRC crystallization plate (ProGENE). Crystals reached a maximal size of 0.20 mm × 0.15 mm × 0.1 mm within 3 weeks. All data sets were collected under cryogenic conditions. Diffraction data for the APH(2″)-IVa−kanamycin A complex were collected on a Rigaku rotating copper anode X-ray generator. A total of 360 images with an oscillation angle of 1° were measured. Diffraction data for the APH(2″)-IVa−tobramycin complex were collected at CMCF beamline 08ID-1 at the Canadian Light Source. A total of 240 images with an oscillation angle of 0.75° were measured at 0.9795 Å. All data sets were processed using the HKL2000 program suite,[25] resulting in the statistics listed in Table 1.

Structure Determination and Refinement. The apo structure of APH(2″)-IVa was determined by molecular replacement with the APH(2″)-IIa−gentamicin complex (PDB entry 3HAM) as the search model using Phaser from the CCP4 suite.[26] A single solution was found and refined with REFMAC[27] when the N- and C-terminal lobes were searched for as separate ensembles. Successive cycles of maximum likelihood refinement, incorporating isotropic temperature-factor and torsion-libration-screw refinement, were alternated with manual adjustments to the model in Coot.[28] TLS refinement was computed with seven subsegments per protein molecule, with all subsegments manually chosen on the basis of secondary structural features. Solvent molecules were subsequently added until no significant improvement in model statistics could be observed. The structure of APH(2″)-IVa bound to tobramycin was determined by molecular replacement with the apo APH(2″)-IVa structure. A single solution was found and refined with REFMAC. A partially refined structure of the APH(2″)-IVa−tobramycin complex was used to determine the binary structure with kanamycin A. The aminoglycoside molecules were added to the model based on difference electron density maps ($F_o - F_c$ and $2F_o - F_c$) and refined on the basis of stereochemical constraints obtained from the PRODRG2 server.[29] Final refinement statistics are listed in Table 1.

RESULTS

Apo Structure. The crystal structure of apo APH(2″)-IVa was determined with one protein molecule per asymmetric unit and has been refined to 2.05 Å resolution, with an R_{factor} of 0.219 and

Table 1. Data Collection and Refinement Statistics

	APH(2″)-IVa	APH(2″)-IVa−tobramycin	APH(2″)-IVa−kanamycin A
resolution range (Å)[a]	23.8−2.05 (2.10−2.05)	34.0−1.80 (1.85−1.80)	50.0−2.15 (2.21−2.15)
space group	$P2_12_12_1$	$P2_1$	$P2_1$
a (Å)	50.9	43.3	42.9
b (Å)	61.7	101.5	101.4
c (Å)	102.9	73.5	73.4
β (deg)		100.8	100.6
no. of reflections	18692	54440	32322
completeness (%)	93.97 (97.2)	99.4 (99.7)	99.7 (98.9)
redundancy	10.9 (7.0)	5.1 (5.1)	7.0 (5.8)
mean $I/\sigma(I)$	37.1 (4.1)	27.4 (4.1)	22.6 (4.6)
R_{sym}[b]	0.057 (0.32)	0.059 (0.35)	0.095 (0.32)
R_{cryst}[c]/R_{free}[d]	0.219/0.262	0.188/0.242	0.198/0.251
no. of non-hydrogen atoms			
protein	2432	4988	4941
substrate	−	64	66
solvent	102	341	175
root-mean-square deviation			
bond lengths (Å)	0.022	0.023	0.021
bond angles (deg)	1.838	1.899	1.871
average thermal factor (Å^2)			
protein	20.99	24.4	23.1
substrate	−	36.1	44.2
solvent	22.36	29.0	22.0
Ramachandran statistics (%)[e]			
most favored regions	89.9	90.0	91.8
additionally allowed regions	9.7	10.0	7.5
generously allowed regions	0.4	0.0	0.7
disallowed regions	0.0	0.0	0.0

[a] Values in parentheses refer to reflections in the highest-resolution shell. [b] $R_{sym} = \Sigma_{hkl}\Sigma_i|I_i(hkl) - \langle I(hkl)\rangle|/\Sigma_{hkl}\Sigma_i I_i(hkl)$, where $\langle I(hkl)\rangle$ is the average intensity of equivalent reflections and the sum is extended over all measured observations for all unique reflections. [c] $R_{cryst} = \Sigma_{hkl}(||F_o| - |F_c||)/\Sigma_{hkl}|F_o|$, where $|F_o|$ is the observed and $|F_c|$ the calculated structure factor amplitude of a reflection. [d] R_{free} was calculated by randomly omitting 5% of the observed reflections from the refinement. [e] According to the Ramachandran plot in PROCHECK.[35]

Figure 1. Crystal structures of APH(2″)-IVa. (A) Crystal structure of apo APH(2″)-IVa in schematic representation. The N-terminal lobe of the enzyme is colored green, the core region yellow, and the thumb region blue. (B) Structural alignment of the apo and tobramycin-bound structures of APH(2″)-IVa in ribbon representation. The apo structure (green) is superimposed on the binary structure (blue) using residues of the core region. The tobramycin molecule is shown in stick representation and colored cyan. (C) Each black line represents the relative shift between corresponding C_α atoms in the apo and tobramycin-bound structures. Figures 1−3 were prepared with PyMOL.[36]

an R_{free} of 0.262 (Figure 1A). The apo structure of APH(2″)-IVa has been recently reported in three crystal forms with resolutions ranging from 2.2 to 2.4 Å,[16] superposition of which revealed that these three forms are essentially identical. The N-terminal lobe

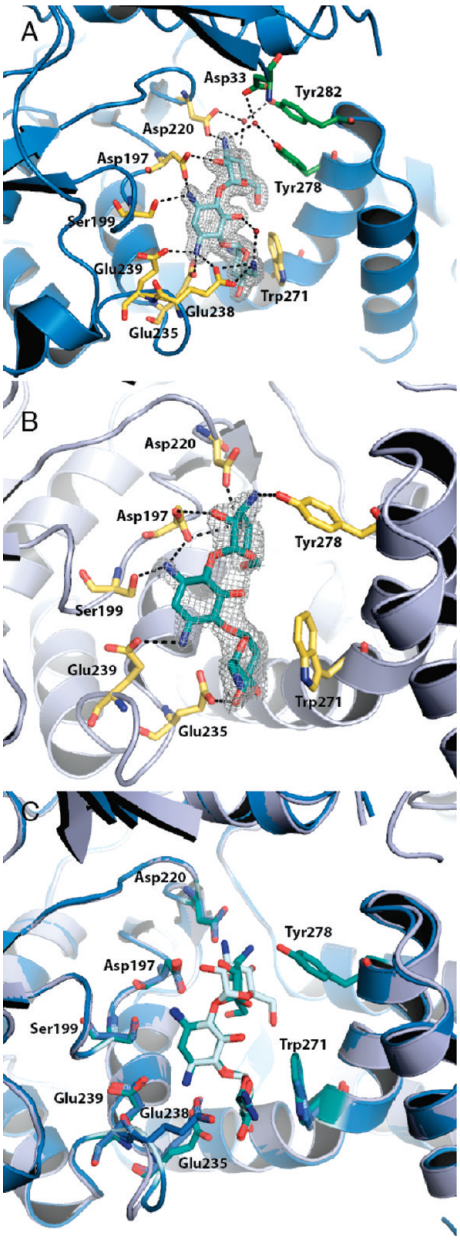

Figure 2. Aminoglycoside-binding site. (A) APH(2″)-IVa—tobramycin complex, showing the $2F_o - F_c$ electron density (gray, 1.0σ) for the tobramycin substrate (cyan stick representation). Hydrogen bonding interactions are represented as black dashed lines. Residues that interact directly with the ligand are shown in stick representation and colored yellow. Ordered water molecules are highlighted as red spheres. Residues that interact indirectly with the ligand via the hydrogen bonding network are shown in stick representation and colored green. (B) APH(2″)-IVa—kanamycin A complex, showing the $2F_o - F_c$ electron density (gray, 1.0σ) for the kanamycin A substrate (green stick representation). (C) Structural superposition of the APH(2″)-IVa—tobramycin complex (blue) onto the APH(2″)-IVa—kanamycin A complex (gray). Residues that form hydrogen bonds with the antibiotic (highlighted in blue for the tobramycin-bound complex and green for the kanamycin A-bound complex) show minimal conformational variation between the two substrate-bound complexes. Tobramycin (cyan) and kanamycin A (green) bind to the protein in very similar conformations, with the only difference being at ring C, which forms a greater angle with respect to ring B in the APH(2″)-IVa—kanamycin A complex.

and the core subdomain are well conserved across all three structures, while several parts of the helical subdomain of one form showed small reorientations compared to the others. Comparisons of our apo structure with the three forms previously published show that it is essentially isomorphous with form I (PDB entry 3N4T). However, while the core subdomain overlaps very well with the previous structures, both the N-terminal lobe and the helical subdomain show relative reorientations. The five-stranded β-sheet in the N-terminal lobe is rotated away from the substrate-binding site, corresponding to a translation of up to 3.0 Å of the loop between β1 and β2 and up to 4 Å of the loop between β4 and β5. In the helical subdomain, traditionally termed the "thumb" region, the largest structural difference is that the long helix α9 bends at a less acute angle, thereby shifting helix α10 and the C-terminal portion of helix α9 away from the aminoglycoside-binding pocket by up to 3.0 Å.

Binary Structures. The APH(2″)-IVa—tobramycin complex has been refined to 1.8 Å with an R_{factor} of 0.188 and an R_{free} of 0.242, while the APH(2″)-IVa—kanamycin A complex has been refined to 2.1 Å with an R_{factor} of 0.198 and an R_{free} of 0.251. Both binary structures were determined in a monoclinic space group with two protein molecules per asymmetric unit, affording a total of four crystallographically independent APH(2″)-IVa—aminoglycoside structures. These represent the first crystal structures of APH(2″)-IVa in complex with a bound antibiotic substrate. The thermal factors for the aminoglycosides, especially for kanamycin A, are higher than those for the protein molecules. Given the inherent structural flexibility of aminoglycosides, ring C may be able to interact with the protein in slightly varying conformations, thereby causing the incomplete occupancy of some atoms of the ligands.

Consistent with other APH structures, the aminoglycoside binds in a cleft formed between the helical and core subdomains of the C-terminal lobe of the protein (Figure 2). Given the abundance of positive charges on this class of antibiotics, it is not surprising that a large number of residues located in the aminoglycoside-binding pocket are acidic in nature. The APH(2″)-IVa—tobramycin complex shows that the antibiotic molecule is positioned in its binding pocket such that the 2″-hydroxyl group of the C ring is 2.8 Å from the $O_{\delta 1}$ atom of the putative catalytic base, Asp197. This residue is part of the catalytic loop widely seen in protein kinases and is conserved among all members of the APH family.[20] Besides Asp197, ring C interacts with only one other side chain, Asp220.

The majority of interactions between the protein and ligand are formed with rings A and B of the aminoglycoside. The 2-deoxystreptamine ring (ring B) is nestled against the core subdomain and interacts with Asp197, Ser199, and three glutamates from the loop between helices α7 and α8 (Glu235, Glu238, and Glu239). Ring A, which is oriented nearly perpendicularly to ring B, is stabilized by Glu238 and Glu239. In addition, ring A is stabilized by a nonpolar stacking interaction with the indole ring of Trp271. It is intriguing to note that, with the exception of the nonpolar interaction with Trp271, all other interactions between the protein and ligand occur at the side of the ligand that faces the core subdomain, or the convex side of the molecule. Although direct interactions on the concave side with the helical subdomain are absent, two well-defined water molecules, as evidenced by below-average temperature factors, bridge the gaps between ring C and Tyr278 and Tyr282. Two other well-defined water molecules interacting with the aminoglycoside are also stabilized by residues Asn32 and Asp33 from the loop between β1 and β2 of the N-terminal lobe.

Comparison between the APH(2″)-IVa−tobramycin (Figure 2A) and APH(2″)-IVa−kanamycin A (Figure 2B) complexes reveals that the aminoglycoside is bound in an almost identical conformation, the only difference being a more pronounced twist in ring C in the APH(2″)-IVa−kanamycin A complex, bringing it nearly perpendicular to ring B and coplanar with ring A (Figure 2C). This twist presents the 3″-amino group in sufficient proximity of the helical subdomain to allow a direct hydrogen bond with Tyr278 without the need for water molecules to bridge the gap. The only structural differences between tobramycin and kanamycin A lie in two functional groups on ring A. Tobramycin has an additional amino group in the 2′-position, and the electrostatic interactions afforded by this group with nearby glutamate residues could explain the 2-fold discrepancy in binding affinity between the two aminoglycosides.[16]

Comparison between Apo and Binary Structures of APH(2″)-IVa. Comparison between the apo and binary protein structures shows conformational changes in both the N-terminal lobe and the thumb region (Figure 1B). The N-terminal lobe twists toward the aminoglycoside-binding pocket, thereby presenting the loop between strands β1 and β2 in a position to interact with the bound aminoglycoside. This twist corresponds to a translation of 4.7 Å for Asn32, bringing it into the proximity of ring C. The helices in the thumb region also show reorientations in the two substrate-bound structures when compared with the substrate-free structure: conformational differences for helix α5 are likely a consequence of crystal packing interactions. In the binary structures, the two protein molecules forming each asymmetric unit come into the proximity of each other. In particular, the side chain hydroxyl group of each Ser140 forms a hydrogen bond with the amide backbone of the same residue in the other molecule, leading to a distortion of the 3_{10}-helix (α4′) and the beginning of α5. Helix α6 is parallel to helix α5 and shows a similar displacement. This observation lends further support to an earlier reported finding that although helices α5 and α6 move as a rigid unit, they form an inherently flexible region of the protein.[17] The conformational variation of residues 277−285 is likely linked to the presence of the substrate in its binding pocket, because the difference in the binary structure sharpens the kink in helix α9, thereby bringing the C-terminal end of this helix into a position to stabilize the 2″-ring of the aminoglycoside antibiotic. In addition to the shift of the helix, the side chain of Tyr278 is also repositioned to point toward the ligand, involving a total displacement of the terminal hydroxyl group of >7 Å and brining it close enough to form hydrogen bonds with Asn32 and Asp33 of the N-terminal lobe. In effect, the conformational changes described above result in a more compact aminoglycoside-binding pocket.

DISCUSSION

Aminoglycoside Preference of APH(2″)-IVa. The crystal structures of the APH(2″)-IVa−tobramycin and APH(2″)-IVa−kanamycin A complexes represent the first binary structures for this enzyme. Together with the APH(3′) subfamily, the APH(2″) enzymes form the only two subfamilies of APHs that are capable of deactivating a wide range of aminoglycoside antibiotics. The substrate specificity of APH(2″)-IVa can be explained by examining its aminoglycoside-binding site architecture, which can also serve as a point of departure for the design of next-generation aminoglycosides.

The large number of interactions and the relative rigidity of the neamine core of the aminoglycoside suggest that large-scale alterations in this portion of the ligand may be poorly tolerated by the enzyme. Amikacin, which is kanamycin A derivatized at the N1 position by a bulky 4-amino-2-hydroxybutyrate functionality, would fit poorly into the binding pocket because of potential steric clashes with nearby side chains of residues from the core subdomain, in particular Asp201, which rationalizes the 30-fold decrease in binding affinity for amikacin compared to that for kanamycin A.[16] The observation that amikacin is nevertheless a weak substrate of APH(2″)-IVa suggests that side chains of Asp201 and His202 are capable of being displaced upon antibiotic binding. The displacement may be facilitated electrostatically because of the abundance of negatively charged residues around the aminoglycoside. Because Asp201 is not otherwise directly involved in any interactions with substrate stabilization in APH(2″)-IVa, it is conceivable that mutants featuring a less bulky residue may exhibit more elevated resistance levels to amikacin. This potential of increasing the substrate promiscuity of APH(2″)-IVa is of clinical concern because amikacin and isepamicin are alternatives currently considered in cases where drug resistance precludes the use of gentamicin against enterococci infections.[30] Kinetic studies have also shown that 4,5-disubstituted aminoglycosides such as neomycin B are not substrates for APH(2″)-IVa but instead are able to act as dead-end inhibitors.[16] Structurally, this can be explained by noting that in 4,5-disubstituted aminoglycosides, A−B−C rings form a much more acute angle, thereby shifting ring C toward the helical subdomain and away from the site of catalysis if rings A and B are bound in the same manner. The demand on space imposed by ring C and an additional ring D may be accommodated given the flexibility of the helical subdomain, and in particular helix α9.

Comparison with Substrate-Bound Structures of Other APHs. Although enzymes of the APH family share structural and topological resemblances, comparison of known binary structures reveals radically different modes of aminoglycoside binding, which can account for the diverse substrate profiles observed. Because APH(2″)-IVa has its unique substrate preference, it would not be a surprise to see key differences in its interactions with the ligand compared to those of even its closest relative, APH(2″)-IIa. Given the large number of interactions between the core subdomain and the aminoglycoside for the latter, it has been posited that the helical subdomain plays an only minor role in substrate binding.[17] The observed conformational changes in APH(2″)-IVa stand in contrast thereof and suggest that the helical subdomain has a more active role in substrate binding.

The importance of the helical subdomain as a determinant of substrate specificity is supported by another member of the APH family, spectinomycin phosphotransferase or APH(9)-Ia. This enzyme confers resistance against one specific antibiotic, and a detailed study of the protein−ligand interactions reveals that most contacts occur with the helical subdomain.[19] A remarkable feature of APH(9)-Ia is a conformational change in the N-terminal lobe and, to a smaller extent, the thumb region upon substrate binding, thereby forming a compact binding pocket. Although domain movements at the scale of APH(9)-Ia are not observed for APH(2″)-IVa, the smaller conformational changes in the N-terminal lobe and the thumb region upon substrate binding (Figure 1C) nevertheless represent a departure from APH(2″)-IIa and APH(3′) enzymes, which rely on a less restrictive binding pocket to accommodate a wide range of

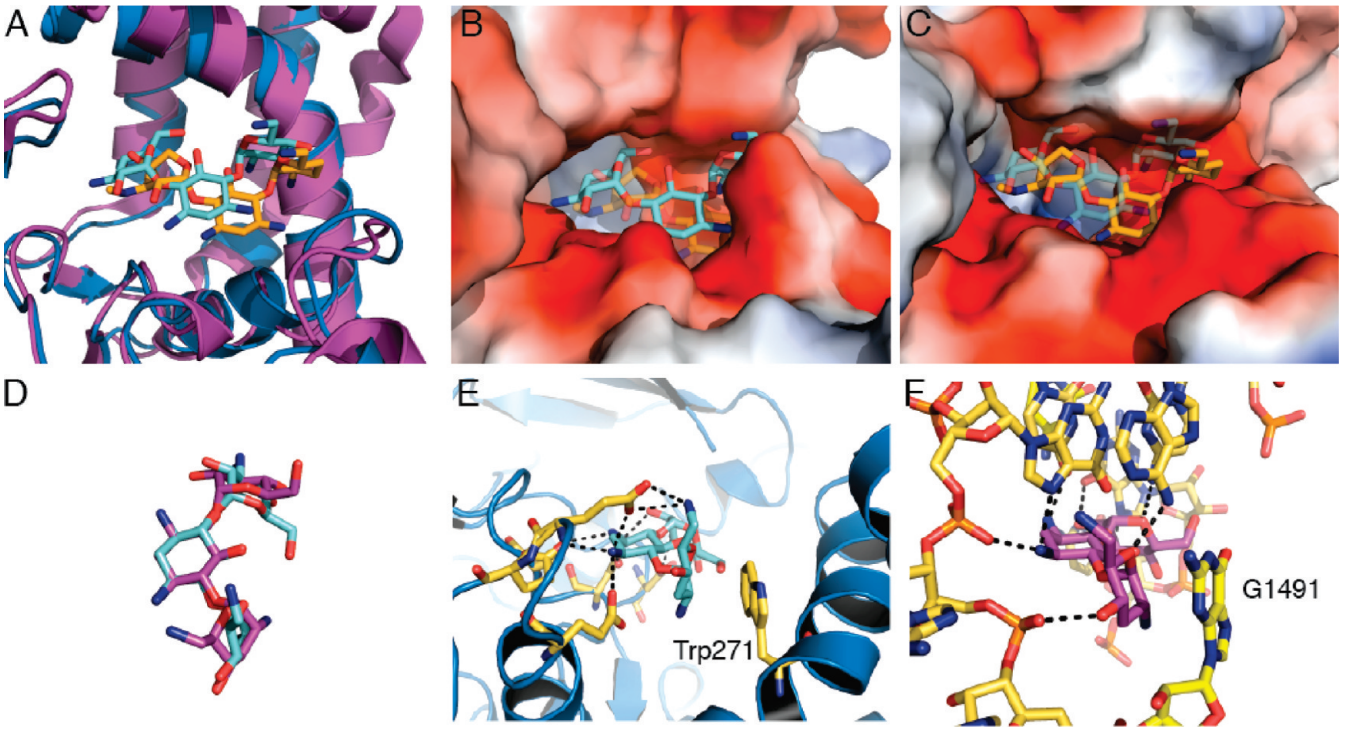

Figure 3. Aminoglycoside-binding site comparisons with APH(2″)-IIa and the ribosomal A-site. (A) Structural superposition of the APH(2″)-IVa−tobramycin complex (colored blue with the substrate in cyan stick representation) onto the APH(2″)-IIa−gentamicin C complex (PDB entry 3HAM, colored purple with substrate in orange representation) using residues of the core region, showing the displacement of the aminoglycoside. (B) Surface representation of the tobramycin-binding site in APH(2″)-IVa with the tobramycin molecule colored cyan. The gentamicin C molecule as bound in APH(2″)-IIa is indicated in transparent orange stick representation. (C) Surface representation of the gentamicin-binding site in APH(2″)-IIa with the gentamicin C molecule colored orange, showing a less compact binding pocket on the concave side of the molecule, in particular around ring C. The tobramycin molecule as bound in APH(2″)-IVa is indicated in transparent cyan stick representation. (D) Superposition of the tobramycin molecules in the conformations in which they bind to APH(2″)-IVa (cyan) and the ribosomal A-site (magenta; PDB entry 1LC4). (E) Transparent surface representation of the aminoglycoside-binding site of APH(2″)-IVa, with the tobramycin molecule in stick representation and colored cyan. Residues that form direct interactions with the ligand (orange) mainly interact with the aminoglycoside from the convex side of the molecule, which corresponds to the core region of the protein. (F) Crystal structure of tobramycin bound to the eubacterial 16S rRNA A-site (PDB entry 1LC4), with the tobramycin molecule in the same orientation as in Figure 3E and colored cyan. Residues that form direct interactions with the ligand (orange) mainly interact with the aminoglycoside from the top face of the molecule.

substrates as opposed to the flexibility of the enzyme itself.[31,32] The interactions observed among Tyr278, Asn32, and Asp33 and their stabilizing effect on the aminoglycoside are absent in the substrate-bound structure of APH(2″)-IIa because of the greater distance between the N-terminal lobe and the aminoglycoside-binding pocket, as well as the less acute angle in helix α9, which pushes residues at the end of the helix farther from the aminoglycoside-binding site. In addition, superposition of substrate-bound forms of APH(2″)-IIa and APH(2″)-IVa shows that the ligand is shifted by approximately 2 Å in the direction of residues from the helical subdomain and the N-terminal lobe in the latter protein−ligand complex, thus facilitating interactions with these regions (Figure 3A). This shift is likely because the shorter side chains of aspartate residues stabilizing rings A and B are replaced with glutamate residues in APH(2″)-IVa. Taken together, these variations result in a more compact binding pocket for APH(2″)-IVa, especially around ring C (Figure 3B, C). In contrast to these two APH(2″) enzymes, APH(2″)-Ia is able to deactivate 4,5-disubstituted aminoglycosides, suggesting that it interacts with its substrate via a yet different method compared to other APH(2″) enzymes characterized thus far. Although detailed analysis of the structural differences between APH(2″)-IVa and APH(2″)-Ia must await the elucidation of the structure of the latter enzyme, our findings thus far show that significant variability in the active site not only is present among APHs that target hydroxyl groups at different positions but also can exist among members of the same subfamily with overlapping substrate profiles. Such variations significantly increase the difficulty in designing generic inhibitors that are potent against a large number of APHs.

Comparison of Aminoglycoside Binding Modes between APH(2″)-IV and the Ribosome. Because APH(2″)-IVa deactivates aminoglycosides that are originally meant to interact with the A-site of the bacterial ribosome, it is instructive to compare the mode of binding of the drug between the intended target and the resistance enzyme. Crystal structures of the entire 30S ribosome in complex with several aminoglycosides were determined in 2000,[5] and subsequently, the crystal structures of tobramycin and kanamycin A in complex with an oligonucleotide containing the A-site have also been determined.[33,34] These structures show similarities as well as striking differences between the mode of binding of the aminoglycoside with the ribosome and that of the resistance enzyme. The stereochemical conformations of the antibiotic molecules in the rRNA binding pocket are similar to those observed for APH(2″)-IVa (Figure 3D), and the majority of interactions between the aminoglycoside and the

A-site also occur with the neamine core portion of the drug. For instance, ring A of tobramycin intercalates in the RNA helix, thus forming a nonpolar stacking interaction with base G^{1491} and a pseudo-base pair with A^{1408}.[33] These interactions are well-mimicked in APH(2″)-IVa, involving the indole ring of Trp271 and the side chain of Glu238, as noted above.

While the majority of functional groups utilized by the aminoglycoside to bind to the ribosome are the same groups that interact with the resistance enzyme, the relative orientations between the drug and its interaction partners exhibit wide differences. In the A-site, the RNA wraps around the antibiotic and most interacting groups extend toward the top face of ring B (Figure 3F). In contrast, key residues from APH(2″)-IVa are mainly situated to the convex side of the molecule and interact with functional groups at the 1-, 3-, 5′-, 2″-, and 3″-positions from a roughly coplanar orientation, which represents a nearly 90° offset from the orientation of the RNA nucleotides (Figure 3E). Binary structures of other members of the APH family, most notably APH(3′)-IIIa, have revealed target mimicry as an effective method of drug inactivation by resistance factors.[31] In the case of APH(3′)-IIIa, target mimicry is achieved by the perpendicular orientation of the face of the aminoglycoside's ring structure relative to its key interacting partners, though the opposite face is used compared to interactions with the A-site. This type of target mimicry is not shown by APH(2″)-IVa, where the enzyme residues project toward the convex edge of the aminoglycoside rings. A necessary consequence of this difference in orientation is that the aminoglycoside is positioned deeper within the enzyme in APH(2″)-IVa. While the antibiotic binding site resembles a relatively shallow pocket in APH(3′)-IIIa, it is a deeper cleft in the APH(2″) enzymes, which may explain the more limited resistance profile of the latter enzymes. The differences in aminoglycoside binding between APH(2″)-IVa and the A-site harbor opportunities for the development of variant aminoglycoside antibiotics that can bind the ribosomal target yet are unable to be inactivated by the resistance protein.

In summary, our structural analysis of the binary complexes of APH(2″)-IVa has highlighted the importance of the helical subdomain in substrate specificity and shown important differences in the mode of aminoglycoside binding between the ribosomal A-site and the resistance factor. Together, these contributions to our general understanding of aminoglycoside phosphotransferases can help in the progress of the rational design of novel next-generation aminoglycoside antibiotics with reduced susceptibility to these resistance factors.

Accession Codes

Atomic coordinates for the apo form of APH(2″)-IVa and its binary complexes with tobramycin and kanamycin A have been deposited in the Protein Data Bank as entries 3SGC, 3SG8, and 3SG9, respectively.

AUTHOR INFORMATION

Corresponding Author

*E-mail: albert.berghuis@mcgill.ca. Telephone: (514) 398-8795. Fax: (514) 398-2036.

Present Addresses

[§]Institute of Structural and Molecular Biology, University of Edinburgh, Edinburgh, U.K.

Funding Sources

This research was supported by a grant from the Canadian Institute of Health Research (Grant MOP-13107) to A.M.B. K.S. is the recipient of a CIHR Banting & Best Graduate Scholarship. A.M.B. holds a Canada Research Chair in Structural Biology.

ACKNOWLEDGMENT

We thank Dr. Joseph Chow for providing us with the *aph(2″)-IVa* gene. We also thank Shaun Labiuk and Pawel Grochulski for data collection at the Canadian Light Source. Finally, we thank past and present members of the A.M.B. lab for their assistance and suggestions, specifically Madhvi Nath. Support for the Canadian Light Source is provided by the Natural Sciences and Engineering Research Council of Canada, the National Research Council Canada, the Canadian Institutes of Health Research, the Province of Saskatchewan, Western Economic Diversification Canada, and the University of Saskatchewan.

REFERENCES

(1) Ramirez, M. S., and Tolmasky, M. E. (2010) Aminoglycoside modifying enzymes. *Drug Resist. Updates 13*, 151–171.

(2) Allison, K. R., Brynildsen, M. P., and Collins, J. J. (2011) Metabolite-enabled eradication of bacterial persisters by aminoglycosides. *Nature 473*, 216–220.

(3) Burk, D. L., and Berghuis, A. M. (2002) Protein kinase inhibitors and antibiotic resistance. *Pharmacol. Ther. 93*, 10.

(4) Moazed, D., and Noller, H. F. (1987) Interaction of antibiotics with functional sites in 16S ribosomal RNA. *Nature 327*, 389–395.

(5) Carter, A. P., Clemons, W. M., Brodersen, D. E., Morgan-Warren, R. J., Wimberly, B. T., and Ramakrishnan, V. (2000) Functional insights from the structure of the 30S ribosomal subunit and its interactions with antibiotics. *Nature 407*, 340–348.

(6) Donabedian, S. M., Thal, L. A., Hershberger, E., Perri, M. B., Chow, J. W., Bartlett, P., Jones, R., Joyce, K., Rossiter, S., Gay, K., Johnson, J., Mackinson, C., Debess, E., Madden, J., Angulo, F., and Zervos, M. J. (2003) Molecular characterization of gentamicin-resistant enterococci in the United States: Evidence of spread from animals to humans through food. *J. Clin. Microbiol. 41*, 1109–1113.

(7) Smith, C. A., and Baker, E. N. (2002) Aminoglycoside antibiotic resistance by enzymatic deactivation. *Curr. Drug Targets: Infect. Disord. 2*, 143–160.

(8) Shaw, K. J., Rather, P. N., Hare, R. S., and Miller, G. H. (1993) Molecular genetics of aminoglycoside resistance genes and familial relationships of the aminoglycoside-modifying enzymes. *Microbiol. Rev. 57*, 138–163.

(9) Mingeot-Leclercq, M.-P., Glupczynski, Y., and Tulkens, P. M. (1999) Aminoglcyosides: Activity and resistance. *Antimicrob. Agents Chemother. 43*, 11.

(10) Kao, S. J., You, I., Clewell, D. B., Donabedian, S. M., Zervos, M. J., Petrin, J., Shaw, K. J., and Chow, J. W. (2000) Detection of the high-level aminoglcoside resistance gene *aph(2″)-Ib* in *Enterococcus faecium*. *Antimicrob. Agents Chemother. 44*, 4.

(11) Badarau, A., Shi, Q., Chow, J. W., Zajicek, J., Mobashery, S., and Vakulenko, S. (2008) Aminoglycoside 2″-phosphotransferase type IIIa from *Enterococcus*. *J. Biol. Chem. 283*, 7638–7647.

(12) Tsai, S. F., Zervos, M. J., Clewell, D. B., Donabedian, S. M., Sahm, D. F., and Chow, J. W. (1998) A new high-level gentamicin resistance gene, *aph(2″)-Id*, in *Enterococcus* spp. *Antimicrob. Agents Chemother. 42*, 1229–1233.

(13) Alam, M. M., Kobayashi, N., Ishino, M., Sumi, A., Kobayashi, K.-I., Uehara, N., and Watanabe, N. (2005) Detection of a novel aph(2″) Allele (*aph[2″]-Ie*) conferring high-level gentamicin resistance and a spectinomycin resistance gene *ant(9)-Ia* (*aad9*) in clinical isolates of Enterococci. *Microb. Drug Resist. 11*, 9.

(14) Abbassi, M. S., Achour, W., and Hassen, A. B. (2007) High-level gentamicin-resistant *Enterococcus faecium* strains isolated from bone marrow transplant patients: Accumulation of antibiotic resistance genes,

large plasmids and clonal strain dissemination. *Int. J. Antimicrob. Agents 29*, 658–664.

(15) Zarrilli, R., Tripodi, M. F., Di Popolo, A., Fortunato, R., Bagattini, M., Crispino, M., Florio, A., Triassi, M., and Utili, R. (2005) Molecular epidemiology of high-level aminoglycoside-resistant enterococci isolated from patients in a university hospital in southern Italy. *J. Antimicrob. Chemother. 56*, 827–835.

(16) Toth, M., Frase, H., Antunes, N. T., Smith, C. A., and Vakulenko, S. B. (2010) Crystal structure and kinetic mechanism of aminoglycoside phosphotransferase-2″-IVa. *Protein Sci. 19*, 1565–1576.

(17) Young, P. G., Walanj, R., Lakshmi, V., Byrnes, L. J., Metcalf, P., Baker, E. N., Vakulenko, S. B., and Smith, C. A. (2009) The crystal structures of substrate and nucleotide complexes of *Enterococcus faecium* aminoglycoside-2″-phosphotransferase-IIa [APH(2″)-IIa] provide insights into substrate selectivity in the APH(2″) subfamily. *J. Bacteriol. 191*, 4133–4143.

(18) Nurizzo, D., Shewry, S. C., Perlin, M. H., Brown, S. A., Dholakia, J. N., Fuchs, R. L., Deva, T., Baker, E. N., and Smith, C. A. (2003) The crystal structure of aminoglycoside-3′-phosphotransferase-IIa, an enzyme responsible for antibiotic resistance. *J. Mol. Biol. 327*, 491–506.

(19) Fong, D. H., Lemke, C. T., Hwang, J., Xiong, B., and Berghuis, A. M. (2010) Structure of the antibiotic resistance factor spectinomycin phosphotransferase from *Legionella pneumophila*. *J. Biol. Chem. 285*, 9545–9555.

(20) Hon, W. C., McKay, G. A., Thompson, P. R., Sweet, R. M., Yang, D. S. C., Wright, G. D., and Berghuis, A. M. (1997) Structure of an enzyme required for aminoglycoside antibiotic resistance reveals homology to eukaryotic protein kinases. *Cell 89*, 887–895.

(21) Stogios, P. J., Shakya, T., Evdokimova, E., Savchenko, A., and Wright, G. D. (2011) Structure and function of APH(4)-Ia, a hygromycin B resistance enzyme. *J. Biol. Chem. 286*, 1966–1975.

(22) Fong, D. H., Xiong, B., Hwang, J., and Berghuis, A. M. (2011) Crystal structures of two aminoglycoside kinases bound with a eukaryotic protein kinase inhibitor. *PLoS One 6*, e19589.

(23) Toth, M., Chow, J. W., Mobashery, S., and Vakulenko, S. B. (2009) Source of phosphate in the enzymic reaction as a point of distinction among aminoglycoside 2″-phosphotransferases. *J. Biol. Chem. 284*, 6690–6696.

(24) McKay, G. A., Thompson, P. R., and Wright, G. D. (1994) Broad spectrum aminoglycoside phosphotransferase type III from *Enterococcus*: Overexpression, purification, and substrate specificity. *Biochemistry 33*, 6936–6944.

(25) Otwinowski, Z., and Minor, W. (1997) Processing of X-ray Diffraction Data Collected in Oscillation Mode. In *Methods in Enzymology* (Carter, C. W. J., and Sweet, R. M., Eds.) pp 307−326, Academic Press, San Diego.

(26) Collaborative Computational Project Number 4. (1994) The CCP4 Suite: Programs for protein crystallography. *Acta Crystallogr. D50*, 760–763.

(27) Murshudov, G. N., Vagin, A. A., and Dodson, E. J. (1997) Refinement of macromolecular structures by the maximum-likelihood method. *Acta Crystallogr. D53*, 2126–2132.

(28) Emsley, P., Lohkamp, B., Scott, W. G., and Cowtan, K. (2010) Features and development of Coot. *Acta Crystallogr. D66*, 486–501.

(29) Schuettelkopf, A. W., and van Aalten, D. M. F. (2004) PRODRG: A tool for high-throughput crystallography of protein-ligand complexes. *Acta Crystallogr. D60*, 1355–1363.

(30) Maviglia, R., Nestorini, R., and Pennisi, M. (2009) Role of old antibiotics in multidrug resistant bacterial infections. *Curr. Drug Targets 10*, 895–905.

(31) Fong, D. H., and Berghuis, A. M. (2002) Substrate promiscuity of an aminoglycoside antibiotic resistance enzyme via target mimicry. *EMBO J. 21*, 2323–2331.

(32) Fong, D. H., and Berghuis, A. M. (2009) Structural basis of APH(3′)-IIIa-mediated resistance to N1-substituted aminoglycoside antibiotics. *Antimicrob. Agents Chemother. 53*, 3049–3055.

(33) Vicens, Q., and Westhof, E. (2002) Crystal structure of a complex between the aminoglycoside tobramycin and an oligonucleotide containing the ribosomal decoding A site. *Chem. Biol. 9*, 747–755.

(34) Vicens, Q., and Westhof, E. (2003) RNA as a drug target: The case of aminoglycosides. *ChemBioChem 4*, 1018–1023.

(35) Laskowski, R. A., MacArthur, M. W., Moss, D. S., and Thornton, J. M. (1993) PROCHECK: A program to check the stereochemical quality of protein structures. *J. Appl. Crystallogr. 26*, 283–291.

(36) *The PyMOL Molecular Graphics System*, version 1.3 (2008) Schroedinger, LLC, New York.